Criticality, tricriticality, and crystallization in discretized models of electrolytes

A. Ciach[1] and G. Stell[2]
[1]*Institute of Physical Chemistry, Polish Academy of Sciences 01-224 Warszawa, Poland*
[2]*Department of Chemistry, State University of New York, Stony Brook, New York 11794-3400, USA*
(Received 30 January 2004; published 15 July 2004)

The Restricted Primitive Model of ionic systems is studied within a field-theoretic approach in order to provide a theoretic basis for the qualitative difference in the phase diagrams obtained in simulations for $\sigma/a=1$, $\sigma/a=2$, and $\sigma/a\geqslant 3$ (a is the lattice constant and σ is the ion diameter). The evolution of the phase diagrams from the case $\sigma/a=1$ to the case $\sigma/a=\sqrt{2}$ [nearest-neighbor (NN) occupancy excluded] is studied in the model with NN repulsion, $0\leqslant J\leqslant\infty$, supplementing Coulomb forces. The boundary of stability of the charge-disordered phase with respect to short-wavelength charge fluctuations and the tricritical point are found in a mean-field (MF) approximation. Next, the effect of fluctuations is studied and we find that for J exceeding a particular value J_0 a fluctuation-induced first-order phase transition should be expected instead of the continuous transition found in MF. At $J=J_0$ the line of continuous transitions splits into two lines enclosing the two-phase region, whose thickness increases from zero when $J\geqslant J_0$ increases. We argue that this transition corresponds to formation of a bcc ionic crystal. For high densities the ions form an fcc crystal, for which we find a fluctuation-induced first-order charge-ordered–charge-disordered transition, in agreement with recent simulation studies. Our results also shed light on the simulation results obtained for an off-lattice ionic system, for which a schematic phase diagram is constructed.

DOI: 10.1103/PhysRevE.70.016114 PACS number(s): 05.70.Jk, 61.20.Qg, 64.60.−i, 82.45.−h

I. INTRODUCTION

In the simplest model of ionic systems, the restricted primitive model (RPM), ions are modeled by uniformly charged hard spheres of charge e and diameter σ. In continuum space the RPM system phase separates into uniform ion-poor and ion-rich phases and the critical point (CP) associated with this phase transition belongs to the Ising universality class, as predicted theoretically [1–4] and confirmed by experiments [5] and simulations [6]. Thanks to the universal nature of critical phenomena, lattice models have been extensively used in simulations and calculations aimed at determination of local properties of phase diagrams of uncharged systems. It was natural to expect that a lattice version of the RPM should give results for the phase diagram near the critical point that mirror those of the continuum-space RPM, just as the Ising-model results accurately describe the criticality of simple fluids. This turned out not to be true [7,8]. Quite surprisingly, when in the RPM the positions of the ions are restricted to the lattice sites of the simple cubic (sc) lattice with the lattice constant $a=\sigma$, then instead of the phase separation into two uniform phases, a line of continuous transitions (λ-line) to a charge-ordered phase (with two oppositely charged sublattices) occurs. The continuous transition terminates at a tricritical point (TCP) and becomes first-order at lower temperatures [1,7–9]. Such phase behavior has also been verified by simulation studies [8,10].

The effect of space discretization on the phase behavior was further studied in Ref.[10], where the ions occupied sites of a finely discretized lattice, with integer $\sigma/a\geqslant 1$. When σ/a changes from 1 to 2 and then from 2 to 3, the phase diagrams change character completely. The phase diagram for $\sigma/a=2$ resembles neither the sc-lattice phase-behavior, nor the off-lattice model phase-diagram. Only first-order transition lines between a diluted, uniform phase and a dense, charge-ordered phase were found, therefore it might be possible that neither critical nor tricritical point is present. For $\sigma/a\geqslant 3$, the behavior characteristic of the continuum case was observed, with a critical-point location converging quickly to the values of $kT\sigma/e^2$ and $\rho\sigma^3$ found in the continuum model for increasing σ/a, and neither a TCP nor a line of charge-ordered–charge-disordered transition were detected for the considered range of densities. So far the evolution of phase diagrams when σ/a increases has not been predicted within any theoretical approach. It is important to explain this evolution in order to understand the fundamental differences between critical phenomena and phase equilibria in uncharged and in ionic systems. This is the purpose of our study here, which was begun in [11].

The lattices with $1<\sigma/a<2$ were not studied in Ref.[10], and it was not clear from that work how the diagrams evolve when σ/a increases from 1 to $\sqrt{2}$, then to $\sqrt{3}$, etc. When $\sigma/a=\sqrt{2}$, the occupancy of the nearest-neighbor sites (NN) is excluded, and when $\sigma/a=\sqrt{3}$, the NN and the second nearest-neighbor sites cannot be occupied simultaneously. We shall refer to the cases $\sigma/a=\sqrt{2}$,$\sigma/a=\sqrt{3}$ and $\sigma/a=2$ as model I, II, and III, respectively. The values of σ/a on the sc lattice and in model I are closer to each other than the corresponding values on the sc lattice and in the other models. However, it is not only the size, but also the shape of the region occupied by an ion, which is important. In model I each ion can have 12 neighbors at the distance of the closest approach, as in continuum, while in model III there are only 6 such neighbors, as on the sc lattice. The above observation suggests that one might expect model I to be closer in behavior to the continuum model. The crossover between the order-disorder transition with the associated TCP, and the

gas-liquid phase separation with the associated CP may occur between the sc lattice and model I, therefore, in the present work we focus on the change of character of phase diagrams between these two models. In order to study the evolution of phase diagrams, we shall consider ions on the sc lattice with repulsive interaction $+J$ between nearest neighbors added to the Coulomb interactions. The model with the soft shell enables us to study the change between the sc lattice and model I in a continuous way when J changes from 0 to ∞, since the infinite repulsion is equivalent to exclusion of simultaneous occupancy of the NN sites.

There is another, important property of model I—the uncharged reference system undergoes a transition to a phase in which only one sublattice (with the fcc structure) is occupied [12–14], which means one can hope to study in this model both its disordered "fluid" and its solid phases. This property of model I is particularly important in view of recent simulation results for the RPM [15–17], which show weakly first order order-disorder transition (between charge-disordered and charge-ordered phases) in the fcc solid. No theoretical description of this transition has been proposed yet. It is partially because direct lattice-gas methods based on the formation of two identical, oppositely charged sublattices [18], valid on bipartite lattices, cannot be applied to the fcc lattice. There are no such limitations within our field-theoretic method used here, however. In order to verify whether the order-disorder transition in the fcc solid is of the same origin as the order-disorder transition observed previously in the sc and the bcc lattice models [8,18–20], we shall study model I for high densities, where the occupied sublattice has the fcc structure.

The fundamental reason for the nonuniversal behavior of the critical phenomena in the RPM has been already explained [21], but the phase diagrams obtained in simulations have not been fully reproduced theoretically [20]. In Refs. [1,20–22] it was shown that the λ-line and the TCP result from instability of the disordered phase with respect to charge-density fluctuations (planar waves) [1,20–22], with the wavevector $\mathbf{k}_b$ corresponding to a microscopic wavelength $2\pi/|\mathbf{k}_b| \approx 2\sigma$. Mean-field (MF) analysis [20] shows that the λ-line and the TCP should be present for any space discretization. Beyond MF the whole spectrum of charge fluctuations, which are coupled to number-density fluctuations, induce the phase separation into uniform ion-diluted and ion-dense phases [1,21,22]. Thus, the uniform, disordered phase may become unstable either with respect to charge ordering, or with respect to separation into two uniform phases. Which transition actually occurs, and which is only metastable, depends on the efficiencies of the relevant fluctuations for a particular space discretization. The positions of the λ-line and the TCP depend very strongly on the microscopic details of the model system and on the approximations used [1,9,20,22,23], therefore we expect that the change of character of the phase transitions is governed by the behavior of the order-disorder transition, and we shall focus on this transition here.

Although MF theory predicts existence of a stable or a metastable TCP for any discretization and in continuum [1,20,22], the stable TCP has been observed in simulations only in the $\sigma/a=1$ case. The metastable TCP (located inside the two-phase region) would be associated with the λ-line in the region of stability of the ion-dense phase [1,20]. No such transition has been observed in simulations for $\sigma/a \geqslant 2$, suggesting that even the metastable TCP disappears. Note, however, that the boundary of stability of the charge-disordered phase is associated with finite-wavelength fluctuations, therefore, a fluctuation-induced first-order phase transition may occur [24]. If this expectation is correct, then it remains to be verified why for some discretizations the transition is fluctuation-induced first order, whereas for $\sigma/a=1$ it is continuous at high temperatures. In order to understand the evolution of the phase diagrams it is necessary to determine how the effect of fluctuations on the order of the charge-ordered–charge-disordered phase-transition depends on the space discretization. Our goal here is to determine the order of this transition as a function of J, i.e., on the path from the sc lattice to model I, and for the order-disorder transition between two fcc solid phases.

In the next section we study the evolution between the sc lattice and model I for low concentrations of ions. Both MF analysis and a discussion of the effects of fluctuations on the order of the order-disorder transition, and their dependence on J are described. Model I at high-densities (fcc solid) is analyzed in Sec. III. We find the boundary of stability of the charge-disorderd phase in MF, and beyond MF we show that the transition is fluctuation-induced first order. The phase behavior of model I at intermediate densities is discussed on a qualitative level in Sec. IV, where the bcc lattice is also considered. Final section contains discussion of the results. In particular, a schematic phase diagram of model I resulting from our study is presented. It agrees with the diagram constructed from simulation results for the continuous RPM [15,17].

II. CHARGED HARD-SPHERES COVERED BY SOFT REPULSIVE SHELLS

A. The model

Hamiltonian of the RPM, supplemented with a repulsion between the ions occupying the NN sites of the sc lattice, has the form

$$H_J = \frac{E_0}{2}\sum_{\mathbf{x}}\sum_{\mathbf{x}'\neq\mathbf{x}} V_c(|\mathbf{x}-\mathbf{x}'|)\hat{s}(\mathbf{x})\hat{s}(\mathbf{x}') + \frac{J}{2}\sum_{\mathbf{x}}\sum_{\mathbf{x}'=\mathbf{x}\pm\mathbf{e}^i}\hat{s}^2(\mathbf{x})\hat{s}^2(\mathbf{x}') - \mu\sum_{\mathbf{x}}\hat{s}^2(\mathbf{x}), \qquad (1)$$

where $\hat{s}=+1,-1,0$ represents the anion, the cation and the solvent respectively, and μ is the chemical potential of the ions. The lattice sites are $\mathbf{x}=x_i\mathbf{e}^i$, where $\mathbf{e}^i$ are the unit vectors on the sc lattice, x_i are integer numbers, $i=1,2,3$, summation convention is used and the distance is measured in a units. The V_c is the dimensionless Coulomb interaction (see the Appendix), and the energy unit is $E_0=e^2a_{nn}^2/Dv_0$, where D, a_{nn}, and v_0 are the dielectric constant of the solvent, the distance between nearest-neighbor sites and the volume per site, respectively. The corresponding dimensionless temperature is $T^E=1/\beta^E=kT/E_0$. $J>0$ is the strength of the repul-

sive shell. For $J=0$ the initial RPM model with $\sigma=a$ is recovered. For finite values of J the model describes charged particles consisting of a hard core and a soft shell—for example, charged colloids covered with polymeric brushes. For $J=\infty$ we obtain model I, because the probability that the nearest-neighbor lattice sites are occupied is $\propto e^{-\beta J}$; hence it vanishes for $J=\infty$. The Hamiltonian of model I has the form

$$H=\frac{E_0}{2}\sum_{\mathbf{x}}\sum_{\mathbf{x}'\neq\mathbf{x},\mathbf{x}\pm\mathbf{e}^{\mathbf{i}}} V_c(|\mathbf{x}-\mathbf{x}'|)\hat{s}(\mathbf{x})\hat{s}(\mathbf{x}')-\mu\sum_{\mathbf{x}}\hat{s}^2(\mathbf{x}). \quad (2)$$

B. Mean-field analysis

Our purpose here is a determination of the boundary of stability of the disordered phase with respect to local fluctuations of concentrations of the two ionic species. We assume for both models the following form of the grand-potential functional in the MF approximation:

$$\Omega=F_h[\rho_\alpha(\mathbf{x})]+\mathcal{U}[\rho_\alpha(\mathbf{x})]-\mu\sum_{\alpha}\sum_{\mathbf{x}}\rho_\alpha(\mathbf{x}), \quad (3)$$

where $\rho_\alpha(\mathbf{x})$ is the local density of the component α, with $\alpha=+,-$ denoting the cations and the anions, respectively. We also introduce the dimensionless charge- and number densities (fraction of the ion-occupied sites), $\phi=\langle\hat{s}\rangle=\rho_+-\rho_-$ and $\rho=\langle\hat{s}^2\rangle=\rho_++\rho_-$, respectively. We assume that the total density (ions+solvent) is fixed and that the system is electrically neutral.

Let us first discuss the second term in (3). $\mathcal{U}[\rho_\alpha(\mathbf{x})]=U[\phi]$ is the electrostatic energy of the system, and in Fourier representation is given by

$$U[\phi]=\frac{E_0}{2}\int_{\mathbf{k}}\tilde{V}(\mathbf{k})\tilde{\phi}(\mathbf{k})\tilde{\phi}(-\mathbf{k}), \quad (4)$$

where tilde refers to the Fourier transform of the corresponding function, $\mathbf{k}=(k_1,k_2,k_3)$ and

$$\int_{\mathbf{k}}\equiv\int_{-\pi}^{\pi}\frac{dk_1}{2\pi}\int_{-\pi}^{\pi}\frac{dk_2}{2\pi}\int_{-\pi}^{\pi}\frac{dk_3}{2\pi}. \quad (5)$$

In real space the function V in (4) is related to the dimensionless Coulomb potential V_c by

$$V(\Delta\mathbf{x})=g(\Delta\mathbf{x})V_c(\Delta\mathbf{x}), \quad (6)$$

where $g(\Delta\mathbf{x})$ is the pair distribution function for two points, $\mathbf{x}$ and $\mathbf{x}+\Delta\mathbf{x}$. In the simplest MF approximation $g=1$ for $|\Delta\mathbf{x}|\geqslant 1$. However, for a strong repulsion between the NN sites the correlations between these sites cannot be neglected. We take into account only correlations between the NN sites, and postulate the following form of g:

$$g(\mathbf{x}-\mathbf{x}')=\begin{cases}0 & \text{if} \quad \mathbf{x}=\mathbf{x}'\\ \exp(-\beta J) & \text{if} \quad \mathbf{x}=\mathbf{x}'\pm\mathbf{e}_i\\ 1 & \text{otherwise}\end{cases}. \quad (7)$$

For $J\to\infty$ the above g reduces to the form corresponding to model I, namely:

$$g(\mathbf{x}-\mathbf{x}')=\begin{cases}0 & \text{if} \quad \mathbf{x}=\mathbf{x}' \quad \text{or} \quad \mathbf{x}=\mathbf{x}'\pm\mathbf{e}^i\\ 1 & \text{otherwise}\end{cases}.$$

The function V can be written as

$$V(\Delta\mathbf{x})=V_c(\Delta\mathbf{x})+V_c(\Delta\mathbf{x})(g(\Delta\mathbf{x})-1). \quad (8)$$

The second term in (8) vanishes except from a very small region. From (8) and (7) and the form of the lattice Coulomb potential in Fourier representation (see the Appendix) we obtain

$$\tilde{V}(\mathbf{k})=2\pi\left[\frac{1}{3(1-\tilde{f}_{sc}(\mathbf{k}))}-V_0^{sc}-6V_1^{sc}\tilde{f}_{sc}(\mathbf{k})p\right], \quad (9)$$

where

$$p=1-\exp(-\beta J), \quad (10)$$

and where the lattice characteristic function $\tilde{f}_{sc}(\mathbf{k})$ and the two constants V_0^{sc}, V_1^{sc} are given in the Appendix.

Let us now discuss the first term in Eq. (3). F_h is the Helmholtz free energy functional of the uncharged reference system, containing the entropy of mixing of the two kinds of ions with the solvent and the energy associated with the NN repulsion J. We assume the simplest local-density approximation

$$F_h=\sum_{\mathbf{x}} f_h(\rho_+(\mathbf{x}),\rho_-(\mathbf{x})), \quad (11)$$

and use the relation

$$\beta\frac{\partial^2 f_h}{\partial\rho_\alpha\partial\rho_\beta}=\frac{\delta^{\mathrm{Kr}}_{\alpha,\beta}}{\rho_\alpha}-c_h(\rho), \quad (12)$$

where $\delta^{\mathrm{Kr}}_{\alpha,\beta}$ is the Kronecker delta, the first term in (12) arises from the ideal-entropy of mixing and $c_h(\rho)$ is the integral of the reference-system Ornstein-Zernike direct correlation function over excluded volume. From (12) we obtain the second derivatives of f_h with respect to the variables ϕ,ρ at $\phi=0,\rho=\rho_0$:

$$\beta\left.\frac{\partial^2 f_h}{\partial\phi^2}\right|_{\phi=0,\rho=\rho_0}=\frac{1}{\rho_0}, \quad (13)$$

$$\beta\left.\frac{\partial^2 f_h}{\partial\rho^2}\right|_{\phi=0,\rho=\rho_0}=\frac{1}{\rho_0}-c_h(\rho_0), \quad (14)$$

and

$$\beta\left.\frac{\partial^2 f_h}{\partial\phi\,\partial\rho}\right|_{\phi=0,\rho=\rho_0}=0. \quad (15)$$

Consistent with the approximation for the pair-distribution function g in Eq. (7), we assume for the reference system the Bethe approximation [25], so that the correlations between the NN sites are not neglected. In the considered case the Bethe approximation leads to the equation [25]

$$e^{\beta\mu}=\frac{\rho}{1-\rho}\left[\frac{(B(\rho)-1+2\rho)(1-\rho)}{(B(\rho)+1-2\rho)\rho}\right]^3, \quad (16)$$

where

$$B(\rho) = \sqrt{1 - 4\rho(1-\rho)p}. \tag{17}$$

Thus, for $\beta\partial^2 f_h/\partial\rho^2 = \partial(\beta\mu)/\partial\rho$ we obtain

$$\beta\frac{\partial^2 f_h}{\partial\rho^2}\bigg|_{\phi=0,\rho=\rho_0} = \frac{1}{\rho_0(1-\rho_0)}\left(\frac{3}{B(\rho_0)} - 2\right). \tag{18}$$

The Eqs. (3)–(18) define the grand-potential Ω introduced in (3).

The equilibrium charge and number densities in the uniform phase, $\phi(\mathbf{x})=0, \rho(\mathbf{x})=\rho_0$, correspond to the global minimum of Ω. Local deviations $\phi(\mathbf{x}), \eta(\mathbf{x})=\rho(\mathbf{x})-\rho_0$, from the average values of the charge- and number densities, respectively, can induce the instability of the uniform phase, when the determinant of the second-derivative of Ω with respect to the fields $\phi(\mathbf{x}), \eta(\mathbf{x})$ is not positive. In this model $\delta^2\Omega/\delta\eta(\mathbf{x})\delta\phi(\mathbf{x}')=0$. The density deviations from the average value, $\eta(\mathbf{x})$, cannot induce the instability of the uniform phase in the absence of the charge fluctuations, since from (3), (18), and (17) we find

$$\tilde{C}^0_{\eta\eta}(\mathbf{k}) = \frac{\delta^2\beta\Omega}{\delta\tilde{\eta}(\mathbf{k})\delta\tilde{\eta}(-\mathbf{k})} = \frac{\delta^2\beta F_h}{\delta\tilde{\eta}(\mathbf{k})\delta\tilde{\eta}(-\mathbf{k})} > 0. \tag{19}$$

The uniform phase is unstable with respect to charge fluctuations $\tilde{\phi}(\mathbf{k})$ when

$$\tilde{C}^0_{\phi\phi}(\mathbf{k}) = \frac{\delta^2\beta\Omega}{\delta\tilde{\phi}(\mathbf{k})\delta\tilde{\phi}(-\mathbf{k})} = \frac{1}{\rho_0} + \beta^E\tilde{V}(\mathbf{k}), \tag{20}$$

vanishes. Boundary of stability of the uniform phase corresponds to $\mathbf{k}=\mathbf{k}_b$ such that the Eq. (20) is satisfied first when the temperature is decreased. At the wave vector $\mathbf{k}=\mathbf{k}_b$ the $\tilde{V}(\mathbf{k})$ assumes a minimum. The corresponding line of instability is

$$S = S_\lambda, \quad S_\lambda = -\tilde{V}(\mathbf{k}_b) > 0. \tag{21}$$

where we have introduced the quantity

$$S = \frac{T^E}{\rho_0}. \tag{22}$$

Note that the form of $\tilde{V}(\mathbf{k})$ and its value at the minimum depend significantly on the form of $g(\Delta\mathbf{x})$ (i.e., on discretization) through the second term in (8).

While for $S > S_\lambda$ the global minimum of Ω is assumed at $\phi=0, \rho=\rho_0$, for $S < S_\lambda$ the Ω assumes the minimum at nonvanishing ϕ and η. For $S - S_\lambda \to 0^-$ the order parameters are [1]

$$\phi(\mathbf{x}) = \Phi\cos(\mathbf{k}_b\cdot\mathbf{x}) \tag{23}$$

and

$$\eta(\mathbf{x}) = \frac{\phi(\mathbf{x})^2}{2\rho_0^2\tilde{C}^0_{\eta\eta}(0)} + O(\Phi^4). \tag{24}$$

For $S - S_\lambda \to 0^-$ we find that at the minimum of Ω

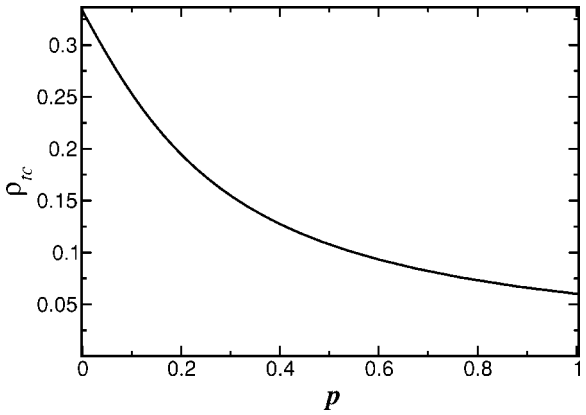

FIG. 1. Density at the TCP, ρ_{tc} as a function of $p=1-\exp(-\beta J)$. All quantities are dimensionless.

$$\frac{1}{4!}\mathcal{A}_4\Phi^2 = \frac{\beta^E}{2}(S_\lambda - S), \tag{25}$$

where terms $O(\Phi^4)$ have been neglected. For all models satisfying (12) we have [20]

$$\mathcal{A}_4 = \frac{1}{\rho_0^3}\left[2 - \frac{3}{\rho_0\tilde{C}^0_{\eta\eta}(0)}\right]. \tag{26}$$

When the coefficient $\mathcal{A}_4$ on the l.h.s. of Eq. (25) becomes negative, the transition between the two phases becomes first order. The TCP is thus given by

$$\mathcal{A}_4 = 0, \quad S = S_\lambda. \tag{27}$$

The density at the TCP as a function of p can be easily obtained from (18) and (26), and the relation between ρ_{tc} and p is given by

$$p = \frac{(7-3\rho_{tc})^2 - 36}{4\rho_{tc}(1-\rho_{tc})(7-3\rho_{tc})^2}. \tag{28}$$

ρ_{tc} as a function of p is shown in Fig. 1. For $p=1$, corresponding to model I, we obtain here $\rho_{tc}\approx 0.0601$.

$\tilde{V}(\mathbf{k})$ given by Eq. (9) assumes a minimum for the wave vectors that satisfy the equation

$$\tilde{f}_{\mathrm{sc}}(\mathbf{k}_b) = \begin{cases} 1 - 2\sqrt{\dfrac{p_0}{p}} & \text{if} \quad p \geqslant p_0 \\ -1 & \text{otherwise} \end{cases}, \tag{29}$$

where

$$p_0 = \frac{1}{72V_1^{\mathrm{sc}}} \approx 0.08 \quad \text{and} \quad J_0 = -kT\log(1-p_0). \tag{30}$$

For $p \leqslant p_0$ $\tilde{V}(\mathbf{k})$ assumes the lowest value at the domain boundary $\mathbf{k}_b = \pi(\pm 1, \pm 1, \pm 1)$, as on the sc lattice ($p=0$), whereas for $p \geqslant p_0$ the Eq. (29) can be written in the form

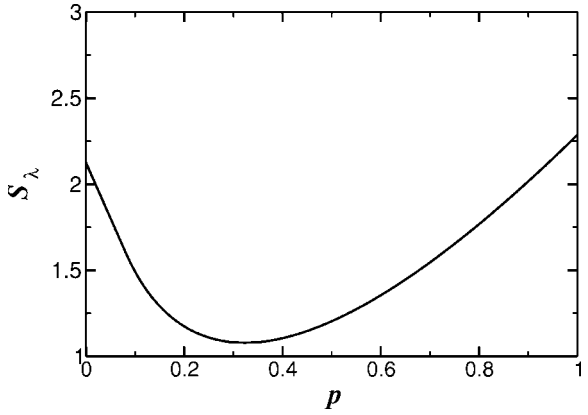

FIG. 2. Slope of the bifurcation line $S_\lambda = T^E/\rho$ as a function of $p = 1 - \exp(-\beta J)$. All quantities are dimensionless.

$$\sum_i^3 \cos k_i^b = 3\left(1 - 2\sqrt{\frac{p_0}{p}}\right). \tag{31}$$

For $p \leqslant p_0$ a unique, well defined structure, i.e., two oppositely charged sublattices, is more stable for $S < S_\lambda$ than the disorderd fluid. For $p \geqslant p_0$ there is a continuum of structures, incommensurate with the lattice, and each of them is equally probable for $S \to S_\lambda^-$, since Ω assumes the same value for any $\mathbf{k}_b$ satisfying Eq. (31) [up to terms $O(\Phi^4)$]. Averaging over all these structures may lead back to the disordered phase. The continuum of incommensurate structures for $p \geqslant p_0$ is related to the fact that the bifurcation vectors $\mathbf{k}_b = (k_1^b, k_2^b, k_3^b)$ occupy a surface, whose area increases from zero when $p \geqslant p_0$ increases. The region occupied by the bifurcation vectors in the $\mathbf{k}$-space plays a major role in the effects of fluctuations on the phase transitions, as will be discussed in the next subsection in more detail.

The slope of the bifurcation line is given by

$$S_\lambda = -\tilde{V}(\mathbf{k}_b) = \begin{cases} -2\pi\left[\frac{1}{6} - V_0^{sc} + 6V_1^{sc}p\right] & \text{if} \quad p \leqslant p_0 \\ -2\pi[2\sqrt{2V_1^{sc}p} - V_0^{sc} - 6V_1^{sc}p] & \text{if} \quad p \geqslant p_0 \end{cases}. \tag{32}$$

S_λ is shown as a function of p in Fig. 2. For model I we obtain the same S_λ as for $p = 1$, by definition of the function g.

It is interesting to compare the results obtained for model I (i.e., $p = 1$) in the Bethe approximation with the results obtained with the help of the more rigorous treatment of the reference system described in Ref. [13]. The reference system (excluded occupancy of the NN sites) undergoes a transition to a nonuniform state at $\rho_0 \approx 0.18$ [13]. In the nonuniform phase two sublattices are formed, with different density at each sublattice; for $\rho_0 > 0.3$ the second sublattice is practically empty. We consider here the low-density regime, i.e., $\rho_0 < 0.18$ and the case of high densities $\rho_0 > 0.3$ is described in Sec. III. The intermediate-density region is discussed in Sec. IV.

The form of $\tilde{C}_{\eta\eta}^0$ for low densities is (see Ref. [13])

$$\tilde{C}_{\eta\eta}^0(0) = \frac{I(y)(1-y)}{\rho_0(1-\rho_0)}, \tag{33}$$

where y is a function of ρ_0 given by $\mathcal{F}(\rho_0, y) = 0$ with

$$\mathcal{F}(\rho_0, y) = I(y) - \frac{1-\rho_0}{1-\rho_0+\rho_0 y}, \tag{34}$$

where

$$I(y) = \int_{\mathbf{k}} \frac{1}{1 - y\tilde{f}_{sc}(\mathbf{k})}. \tag{35}$$

From the condition $\mathcal{A}_4 = 0$, Eq. (25) and from the above the density at the TCP can be obtained numerically and the result is

$$\rho_{tc} = 0.0608, \tag{36}$$

i.e., it is very close to the result obtained within the Bethe approximation.

In the standard reduced RPM units $T^* = kTD\sigma/e^2$ and $\rho^* = \rho v/v_0$, where σ should be identified with the distance of the closest approach between the ions, a_{nn}, and v is the volume per ion, respectively. In the system described by the Hamiltonian (2) the distance of the closest approach is $\sigma = \sqrt{2}a$ and the volume per ion is $v = 2a^3 = 2v_0$, thus the standard dimensionless quantities defined for the RPM are related to T^E and ρ_0 defined above by $T^* = \sqrt{2}T^E$ and $\rho^* = 2\rho_0$, hence

$$\rho_{tc}^* \approx 0.12. \tag{37}$$

Note that ρ_{tc}^* is quite close to $\rho_{tc}^* \approx 0.1$, the value obtained within analogous theory [20] for the continuum RPM using a Percus-Yevick reference-system approximation. The bifurcation line is (see (32)) $T^E/\rho_0 = S_\lambda = -\tilde{V}(\mathbf{k}_b) \approx 2.29$ and in the RPM reduced units $S_\lambda^* \approx 1.62$, i.e., very close to $S_\lambda^* \approx 1.61$ found in the continuous RPM [20]. Thus, for model I the λ-line and the TCP are very close to the results obtained in the continuous system on the same level of the MF approximation.

C. Role of fluctuations

The actual instability with respect to charge-density waves occurs at the highest S such that for some wave vector $\mathbf{k}_b$ the charge-charge correlation function $\langle\tilde{\phi}(\mathbf{k}_b)\tilde{\phi}(-\mathbf{k}_b)\rangle$ diverges, where the probability distribution for $\tilde{\phi}(\mathbf{k})$ is proportional to the Boltzmann factor $\exp(-\beta\Omega)$. In the MF approximation $\langle\tilde{\phi}(\mathbf{k})\tilde{\phi}(-\mathbf{k})\rangle^{MF} = \tilde{G}_{\phi\phi}^0(\mathbf{k}) = 1/\tilde{C}_{\phi\phi}^0(\mathbf{k})$ with $\tilde{C}_{\phi\phi}^0(\mathbf{k})$ defined in (20), i.e., terms beyond the Gaussian part of Ω are neglected in calculating $\langle\tilde{\phi}(\mathbf{k})\tilde{\phi}(-\mathbf{k})\rangle$. Ω is a functional of two fields, $\phi(\mathbf{x})$ and $\eta(\mathbf{x}) = \rho(\mathbf{x}) - \rho_0$. Following Refs. [1,21,22], we minimize Ω for fixed ϕ with respect to η and expand Ω about the minimum at $\eta(\mathbf{x}) = \eta_0(\mathbf{x}) \propto \phi^2(\mathbf{x})$. We obtain a functional of $\phi(\mathbf{x})$ and $\Delta\eta(\mathbf{x}) = \eta(\mathbf{x}) - \eta_0(\mathbf{x})$. The correlations $<\Delta\eta(\mathbf{x})\Delta\eta(\mathbf{x}')>$ are strictly short-range, and the dependence of Ω on $\Delta\eta(\mathbf{x})$ can be neglected when the order-disorder transition is studied. The resulting effective

functional $\Omega_{\rm eff}[\phi]=\Omega[\phi,\eta_0]$, contains in addition to the Gaussian part the dominant contribution of the form $\Omega_{\rm int}[\phi]=(\mathcal{A}_4/4!)\Sigma_{\mathbf{x}}\,\phi^4(\mathbf{x})$. Inclusion of the higher-order terms in $\Omega_{\rm eff}$ leads to additional contributions to $\langle\tilde{\phi}(\mathbf{k})\tilde{\phi}(-\mathbf{k})\rangle$ beyond MF. Let us focus on terms $\Sigma_n\, a_n\mathcal{G}_0^n$, where

$$\mathcal{G}_0=\int_{\mathbf{k}}\tilde{G}^0_{\phi\phi}(\mathbf{k}), \tag{38}$$

and neglect the remaining contributions to $\langle\tilde{\phi}(\mathbf{k})\tilde{\phi}(-\mathbf{k})\rangle$ in the perturbation expansion about the Gaussian solution. The position of the λ-line beyond MF can be obtained within self-consistent Hartree approximation [24,26,27], but our purpose here is a determination of the order of the transition. $\langle\tilde{\phi}(\mathbf{k})\tilde{\phi}(-\mathbf{k})\rangle$ cannot be expanded about the MF solution when $\mathcal{G}_0$ diverges, and the MF approximation breaks down in this case. For diverging $\mathcal{G}_0$ a first-order phase transition is expected [24,26,27] instead of the continuous transition. This expectation has been verified by MC simulations for the Coulomb-frustrated Ising ferromagnet [28,29]—a model very similar to the present model, except that instead of NN repulsion a NN attraction is present. In order to verify whether the transition to the charge-ordered phase is fluctuation-induced first-order, we shall estimate $\mathcal{G}_0$ for $S\to S_\lambda$. The integrand $\tilde{G}^0_{\phi\phi}(\mathbf{k})$ [Eq. (20)] can be written in the form [see (21) and (22)]

$$\tilde{G}^0_{\phi\phi}(\mathbf{k})=\frac{T^E}{S+\tilde{V}(\mathbf{k})}=\frac{T^E}{\tau^0+\Delta\tilde{V}(\mathbf{k})}, \tag{39}$$

where the critical parameter is defined by

$$\tau^0=S-S_\lambda, \tag{40}$$

and $\Delta\tilde{V}(\mathbf{k})=\tilde{V}(\mathbf{k})-\tilde{V}(\mathbf{k}_b)$. The integrand $\tilde{G}^0_{\phi\phi}(\mathbf{k})$ diverges when $\tau^0=0$ and $\mathbf{k}\to\mathbf{k}_b$, and $\mathcal{G}_0$ can be regular or singular, depending on the form of $\Delta\tilde{V}(\mathbf{k})$.

Since $\tilde{V}(\mathbf{k})$ depends only on cos k_i, the integral in $\mathbf{k}$ space can be reduced to a smaller domain $0\le k_i\le\pi$, i.e., $\int_{\mathbf{k}}\equiv 8\int_0^\pi(dk_1/2\pi)\int_0^\pi(dk_2/2\pi)\int_0^\pi(dk_3/2\pi)=8\int'_{\mathbf{k}}$. In order to see whether $\mathcal{G}_0$ is finite, we should estimate the contribution to the integral coming from the neighborhood of $\mathbf{k}_b$, where $\tilde{G}^0_{\phi\phi}(\mathbf{k})$ diverges when $\tau^0=0$.

D. $\mathcal{G}_0=\int_{\mathbf{k}}\tilde{G}^0_{\phi\phi}(\mathbf{k})$ for $p\le p_0$

In the domain $0\le k_i\le\pi$ there is a single bifurcation vector $\mathbf{k}_b=k_b(1,1,1)$ in this case, and because $\tilde{V}(\mathbf{k})$ assumes a minimum at $\mathbf{k}=\mathbf{k}_b$, for $\mathbf{k}\approx\mathbf{k}_b$ $\tilde{G}^0_{\phi\phi}(\mathbf{k})$ can be written in the form

$$\tilde{G}^0_{\phi\phi}(\mathbf{k})=\frac{T^E}{\tau^0+\Delta k_i a_{ij}\Delta k_j+O(k^4)}, \tag{41}$$

where $\Delta k_i=k_i-k_i^b$ and $2a_{ij}$ is the second-derivative matrix of $\tilde{V}(\mathbf{k})$ at $\mathbf{k}_b$. It is easy to see that $\mathcal{G}_0$ assumes a finite value for $\tau^0=0$. Hence, the expansion about the MF result remains valid, the Brazovskii argument [24] cannot be applied and the transition may remain continuous beyond MF. More detailed renormalization-group (RG) analysis [30] shows that the fixed point of the RG flow equations is stable, and the transition indeed remains continuous as long as $p\le p_0$.

E. $\mathcal{G}_0=\int_{\mathbf{k}}\tilde{G}^0_{\phi\phi}(\mathbf{k})$ for $p>p_0$ and in continuum case

Consider a general case with the bifurcation vectors forming a surface of finite area, given by the equation

$$P(k_1,k_2,k_3)=p_b. \tag{42}$$

For example, in continuum Eq. (42) becomes the equation of a sphere, and for model I Eq. (42) is explicitly given by Eq. (31). In this case we can write

$$\mathcal{G}_0\approx\int\frac{dpS(p)}{\tau^0+c(p-p_b)^2}, \tag{43}$$

where $S(p)$ is the area of the surface given by $P(k_1,k_2,k_3)=p$, c is a constant and terms of higher order in the expansion of $\Delta\tilde{V}$ have been neglected. When $S(p)$ is continuous at p_b and $S(p_b)$ is finite, as is the case for sufficiently large $p-p_0$, model I and in continuum, the integral diverges for $\tau^0\to 0$. The Brazovskii argument can be directly applied, and the transition is fluctuation-induced first order for $p>p_0$. Moreover, the transition should occur for $S<S_\lambda$, i.e., below the line of instability found in MF [24,27,29].

III. MODEL I IN THE HIGH DENSITY REGIME–fcc SUBLATTICE

For high densities, $\rho_0>0.3$, the reference system forms an ordered structure, and only one sublattice is occupied, i.e., only the lattice points $\mathbf{x}=x_i\mathbf{e}^i$ whose coordinates in a-units are

$$(i+j,i+k,j+k),\quad (\text{fcc}), \tag{44}$$

where i,j,k are integer, are not empty. The empty sublattice, formed by the nearest-neighbors of the above points, can be disregarded. The occupied lattice has the fcc structure, with the linear size of the unit cell $a_{\rm fcc}=2a$. At the fcc lattice $a_{nn}=\sqrt{2}a=\sigma$ and $v_0=2a^3=v$, hence the temperature and density in reduced units are $T^*=\sqrt{2}T^E$ and $\rho^*=\rho_{\rm fcc}$. At the fcc sublattice the sites are occupied independently of each other, and for the reference system we can assume the form of F_h corresponding to the ideal entropy of mixing. Hence, $\tilde{C}_{\eta\eta}(0)=[\rho_{\rm fcc}(1-\rho_{\rm fcc})]^{-1}$ and the density at the TCP is $\rho_{\rm fcc}=1/3$ [see (26)]. The density at the TCP on the original sc lattice would be $\rho_0=\rho_{\rm fcc}/2=1/6$, which lies outside the considered density interval, hence the transition remains continuous in the solid phase in MF. In this case, for the lattice sites (44) only multiple occupancy is excluded, and we assume

$$g(\mathbf{x}-\mathbf{x}')=\begin{cases}0 & \text{if} \quad \mathbf{x}=\mathbf{x}'\\ 1 & \text{otherwise}\end{cases}. \tag{45}$$

The form of $\tilde{V}(\mathbf{k})$ is thus

$$\tilde{V}(\mathbf{k}) = 2\pi\left[\frac{1}{3(1-\tilde{f}_{\mathrm{fcc}}(\mathbf{k}))} - V_0^{\mathrm{fcc}}\right], \tag{46}$$

where $\tilde{f}_{\mathrm{fcc}}(\mathbf{k})$ and V_0^{fcc} are given in the Appendix.

The bifurcation vector is determined by the lowest value of $\tilde{f}_{\mathrm{fcc}}(\mathbf{k})$. Simple algebra shows that the lowest value of $\tilde{f}_{\mathrm{fcc}}(\mathbf{k})$ is assumed for

$$\mathbf{k}_b = (0,\pi,q). \tag{47}$$

All the vectors obtained by permutations of the coordinates of the above $\mathbf{k}_b$ are also the bifurcation vectors and induce the instability of the disordered phase. All wave vectors lead to the same value of Ω for $S \to S_\lambda$ from below. The slope of the λ-line is $S_\lambda = T^E/\rho_{\mathrm{fcc}} = -\tilde{V}(\mathbf{k}_b) \approx 1.245$, and $S_\lambda^* \approx 1.76$.

Let us examine the structure given by the vector $\mathbf{k}_b = (0,\pi,q)$ and $-\mathbf{k}_b$ in real space. The general form of the corresponding charge-density is

$$\phi(\mathbf{x}) = \Phi \int_{\mathbf{k}} e^{-i\mathbf{k}\cdot\mathbf{x}}[w\delta(\mathbf{k}-\mathbf{k}_b) + w^*\delta(\mathbf{k}+\mathbf{k}_b)], \tag{48}$$

where w^* is the complex conjugate to w and $ww^*=1$. On the fcc lattice the charge density ϕ for $\mathbf{k}_b=(0,\pi,q)$, in the real space representation has the form

$$\phi(\mathbf{x}) = (-1)^{i+k}[w_r \cos[q(j+k)] + w_i \sin[q(j+k)]]\Phi, \tag{49}$$

where w_r and w_i denote the real and the imaginary part of w, respectively, and the coordinates of $\mathbf{x}$ are given in Eq. (44). Note that the structure is incommensurate with the lattice except for $q=\pi/n$, where n is integer. For a particular choice of q, namely $q=\pi/2$ and for $w=(1+i)/\sqrt{2}$, the structure is the same as the one obtained in the continuum RPM [15] for the charge-ordered phase (Fig. 3). Thus, although our analysis concerns only the boundary of stability of the charge-disordered fcc phase, we have shown that the charge-ordering leading to the structure found in simulations induces instability of the charge-disordered phase.

Let us determine the effect of fluctuations on the order of the considered phase transition. We need to find out whether $\mathcal{G}_0 = \int_{\mathbf{k}} \tilde{G}^0_{\phi\phi}(\mathbf{k})$ diverges or not. For $\tilde{V}^{\mathrm{fcc}}$ given by (A1) with (A3) and the line of bifurcation vectors given by (47) we obtain for $\mathbf{k}$ close to this line the approximation

$$\tilde{G}^0_{\phi\phi}(\mathbf{k}) = \frac{T^E}{\tau^0 + \frac{\pi}{32}(1-\cos 2\alpha \cos q)k^2 + O(k^4)}, \tag{50}$$

where $\mathbf{k}=(k\cos\alpha, \pi - k\sin\alpha, q)$, $0 \leqslant \alpha \leqslant \pi/2$ and k is small. By using the cylindrical variables (k,α,q) one can easily verify that $\mathcal{G}_0$ diverges for $\tau^0 \to 0$. This indicates that the transition is fluctuation-induced first order.

IV. MODEL I AT INTERMEDIATE DENSITIES; bcc SUBLATTICE

Let us focus on $T \to 0$. In an open system the ground state depends on μ and is determined by the minimum of $U[\phi]/V - \mu\rho_0$. Here ρ_0 denotes a fraction of occupied cells. If the NN occupancy is excluded, the high-density, charge-ordered structure corresponds to the fraction of occupied cells $\rho_0 = 1/2$ and is shown in Fig. 3. At $\rho_0 = 1/4$ another ordered structure occurs for $T \to 0$, namely only the sites with coordinates

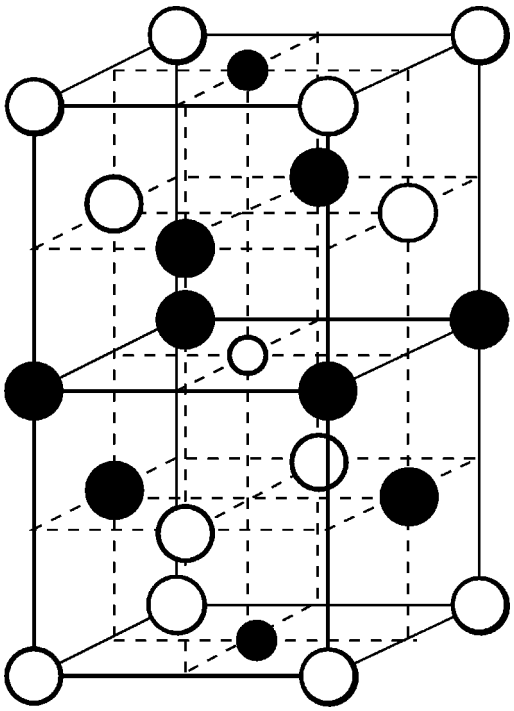

FIG. 3. Structure of the charge-ordered phase on the fcc lattice, with the wavevector $\mathbf{k}_b=(0,\pi,\pi/2)$ and with $w=(1+i)\sqrt{2}$. Black and open circles represent the positive and the negative charges, respectively. See Sec. III A 2 for more details.

$$(i+j-k, i-j+k, -i+j+k), \quad (\mathrm{bcc}), \tag{51}$$

where i,j,k are integer, are occupied. These sites form a bcc sublattice, with the lattice constant of the unit cell $a_{\mathrm{bcc}} = 2a = 2$. The bcc lattice splits into two sublattices, one positively, the other one negatively charged. The first sublattce contains the site $(0,0,0)$, the site $(1,1,1)$ belongs to the other one. At very low T and for $\rho_0 \approx 1/4$ one should expect stability of the bcc charge-ordered solid, whose electrostatic energy is low, then bcc–gas (vacuum) phase coexistence at lower densities, and bcc–fcc phase coexistence at higher densities.

Since the stability of the charge-ordered bcc structure can be expected at low T for intermediate densities, it is instructive to consider the order-disorder transition on the bcc sublattice. In MF we can find the boundary of stability of the charge-disordered phase on the bcc lattice easily. We shall assume that only the lattice sites (51) are occupied, and the remaining, empty sites will be disregarded. We find the λ-line in the same way as in the case of the fcc sublattice, with ρ_{bcc} denoting the fraction of the occupied bcc sites. The fraction of the occupied sites on the original, sc lattice is thus $\rho_0 = \rho_{\mathrm{bcc}}/4$. The bcc sites are occupied independently of each other, hence $\tilde{C}_{\eta\eta}(0) = [\rho_{\mathrm{bcc}}(1-\rho_{\mathrm{bcc}})]^{-1}$ and the density at the

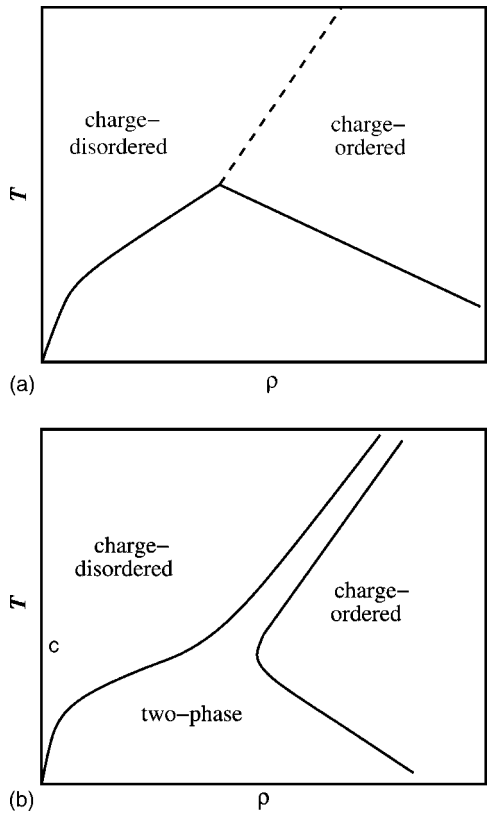

FIG. 4. Schematic representation of the transition between the charge-disorderd and charge-ordered phases. (A) The transition is continuous above the TCP. Such a diagram is expected in a presence of weak NN repulsion $0 \leqslant p < p_0$. (B) The transition is fluctuation-induced first-order. Such a behavior is expected when strong NN repulsion, $p > p_0$, is present, in model I, in continuum and on the fcc lattice. See text for more details.

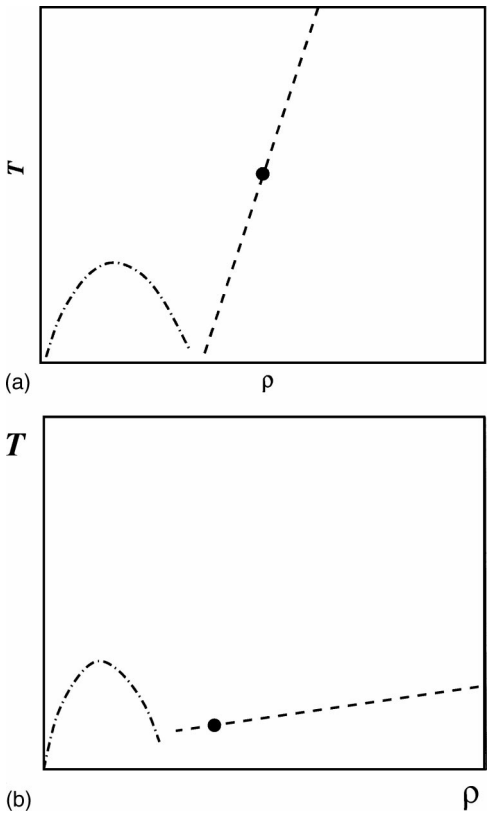

FIG. 5. Spinodal line obtained in Refs. [1,21,22], shown schematically. Dashed line is the boundary of stability of the disordered phase with respect to charge-density fluctuations with the wavelength $\mathbf{k}_b$, black dot is the MF TCP and dash-dotted line is the boundary of stability of the disordered phase with respect to separation into two uniform ion-diluted and ion-dense phases. (A) Such a shape of the spinodal is expected when the fluctuations have a weak disordering effect. We expect such a spinodal line for $p < p_0$. (B) Such a shape of the spinodal is expected when the fluctuations have a strong disordering effect. We expect such a spinodal line for $p > p_0$ and in off-lattice system.

TCP is $\rho_{\mathrm{bcc}} = 1/3$ [see (26)]. The density at the TCP on the original sc lattice would be $\rho_0 = \rho_{\mathrm{fcc}}/4 = 1/12$. As on the fcc sublattice, only multiple occupancy of lattice sites is excluded, and $g(\mathbf{x})$ is given by Eq. (45). The form of $\tilde{V}(\mathbf{k})$ is thus

$$\tilde{V}(\mathbf{k}) = 2\pi \left[\frac{1}{3[1 - \tilde{f}_{\mathrm{bcc}}(\mathbf{k})]} - V_0^{\mathrm{bcc}} \right], \tag{52}$$

where $\tilde{f}_{\mathrm{bcc}}(\mathbf{k})$ and V_0^{bcc} are given in the Appendix. The bifurcation vector is determined by the lowest value of $\tilde{f}_{\mathrm{bcc}}(\mathbf{k})$, which for $\tilde{f}_{\mathrm{bcc}}(\mathbf{k})$ given in Eq. (A4) is $\tilde{f}_{\mathrm{bcc}}(\mathbf{k}_b) = -1$, and is assumed for

$$\mathbf{k}_b = (0,0,\pm\pi), \quad (0,\pm\pi,0), \quad (\pm\pi,0,0), \quad (\pm\pi,\pm\pi,\pm\pi). \tag{53}$$

The slope of the λ-line is $S_\lambda = T^E/\rho_{\mathrm{bcc}} = -\tilde{V}(\mathbf{k}_b) \approx 1.87$, and

$$S_\lambda^* = T^*/\rho^* = \frac{3\sqrt{2}S_\lambda}{2} \approx 3.98, \tag{54}$$

where we have used $a_{nn} = \sqrt{3}$ and $v_0 = 4$ for the bcc lattice, and $\sigma = \sqrt{2}$ and $v = 2$ for model I; hence, $T^* = 3\sqrt{2}T^E/4$ and $\rho^* = \rho_{\mathrm{bcc}}/2 = 2\rho_0$. Note that for the bcc lattice the value of S_λ^* is larger than the corresponding values for the fcc and sc lattices and in off-lattice model.

In the context of model I we can compare stability of the disordered, "fluid" phase and the two bcc solid phases, one charge-ordered, the other one charge-disordered. This phase is stable, whose Ω/V assumes the lowest minimum. The locus of points on the phase diagram where two minima are of equal depth corresponds to the phase transition (the third minimum vanishes or is higher). At T higher than the order-disorder transition temperature on the bcc sublattice the bcc charge-disordered phase is more stable than the charge-ordered phase. However, the stability of the charge-disordered phases is entirely determined by the uncharged reference system for model I. In the latter the stability of the bcc solid (bcc sublattice occupied) is not expected. We can conclude that the charge-ordered–charge-disordered transition line on the bcc lattice forms an upper bound for the stability region of the charge-ordered bcc solid. Moreover, the actual transition between fluid and the bcc charge-ordered solid should be first order. In view of the above

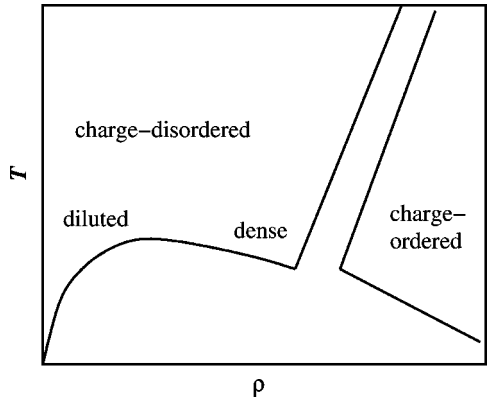

FIG. 6. Low-density part of the phase diagram, expected for $p > p_0$.

discussion it is plausible that the fluctuation-induced first-order transition between a disordered fluid and a charge-ordered phase is identical with the liquid–bcc-solid transition.

V. CONCLUSIONS

We have shown that the line of continuous transitions to a charge-ordered phase with an associated TCP can be transformed continuously into the first-order transition. The change of character of phase diagrams occurs on an sc lattice, when the strength of the NN repulsion ($0 \leqslant J \leqslant \infty$), added to the Coulomb interactions, increases. For $J < J_0$ the uniform phase is unstable along the λ-line with respect to charge-density fluctuations leading to a unique structure, i.e., to two oppositely charged sublattices. The unique structure occurs when the wave vectors of the critical fluctuations are $\mathbf{k}_b = \pi(\pm 1, \pm 1, \pm 1)$, i.e. form vertices of the cubic domain in $\mathbf{k}$-space. For $J = J_0$ the line of continuous transitions to the charge-ordered phase starts to split into two lines enclosing the two-phase region, whose width increases with increasing $J > J_0$. The first-order transition occurs when the disordered phase is unstable with respect to charge-density waves leading to a continuum of charge-ordered structures. Each particular structure is characterized by a wave vector $\mathbf{k}_b$ belonging to a surface of finite area in $\mathbf{k}$-space [Eq. (31)], and for $S \to S_\lambda$ the grand potential for all these structures assumes the same value, hence they occur with the same probability. Averaging over all those structures restores the disordered phase. Only for sufficiently large value of $S_\lambda - S$ the grand potential of a particular, ordered phase vanishes beyond MF for a finite amplitude of the charge density, signaling the first order transition. Such transitions were found before for different models, in which $k \neq 0$ for the critical modes [26–29]. From the analysis described in Sec. IV it follows that the charge-ordered phase which becomes stable for a sufficiently small value of S should have the bcc structure. The two types of the order-disorder transition are shown schematically in Fig. 4. The diagram shown in Fig. 4(A) is consistent with the simulation result for the sc lattice, and the diagram shown in Fig. 4(B) is consistent with the simulation results for $\sigma/a = 2$. [8,10]. The effects of fluctuations on the order of the order-disorder transitions for $\sigma/a = 2$ are described in Ref. [30].

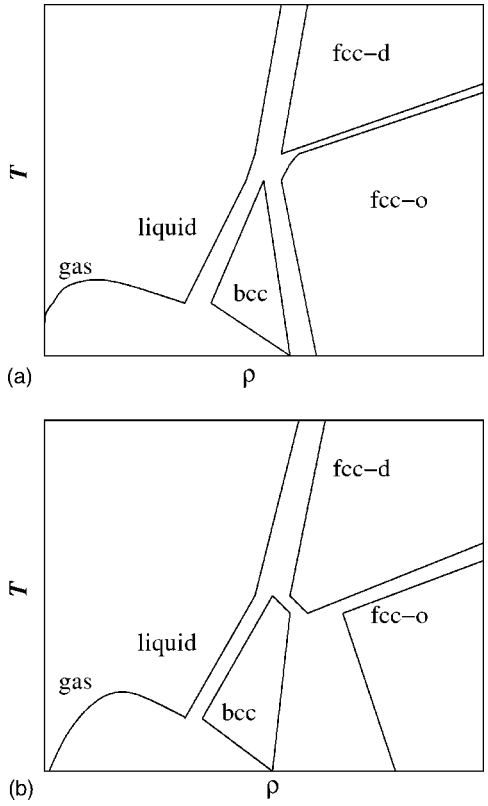

FIG. 7. Schematic phase diagram for model I and for off-lattice models. The present analysis is not sufficient to determine the high-density part of the diagram with sufficient precision. The diagram has the form shown either in (A) or in (B). See text for more explanation.

In addition to the order-disorder transition a phase separation into two uniform, ion-poor and ion-rich phases can take place. It is because the instability of the disordered phase is induced either by $\phi(\mathbf{x}) \propto \cos(\mathbf{k}_b \cdot \mathbf{x})$ or by the whole spectrum of the charge fluctuations, since each charge fluctuation induces the shift of the number density of ions $\eta(\mathbf{x}) \propto \phi^2(\mathbf{x})$ [1,21]. The latter instability can be found after the charge fluctuations are integrated out [1,21,22], and has not been considered in this work. The spinodal line is expected to consist of two parts. The low-density part of the spinodal (dash-dotted line in Fig. 5) describes the instability with respect to phase separation into two uniform (charge-disordered) phases, as found in Refs. [1,3,22]. The position of the spinodal line associated with the phase separation into uniform phases depends on the presence and the kind of the underlying lattice rather weakly [18]. In contrast, the position of the boundary of stability of the uniform phase with respect to the charge-ordering depends crucially on the presence and the kind of the underlying lattice. The slope of this line is different on different lattices in MF (note that fluctuations lead to lower values of S_λ than found in MF). In the presence of the NN repulsion both S_λ and the density at the TCP decrease with J, as shown in Figs. 1 and 2. Schematic representation of the two branches of the spinodal for small and large values of J are shown in Figs.5(A) and 5(B), re-

spectively. If the spinodal has the shape shown in Fig. 5(A), then the CP remains metastable. However, when the spinodal has the form shown in Fig. 5(B), then the critical point associated with the separation into two uniform phases becomes stable. For small values of J the phase diagram should have the form shown in Fig. 4(A), and for $J > J_0$ we expect that the phase diagram should have the form shown schematically in Fig. 6.

For model I we are able to sketch a schematic phase diagram for the whole range of densities, combining the MF predictions for low and high densities presented in Secs. II B and III, respectively, the analysis of the effects of fluctuations (Secs. II B and III) and the analysis of the order-disorder transition on the bcc sublattice (Sec. IV). The result is shown in Fig. 7. At high densities the fcc solid is stable. It undergoes a first-order transition between the high-temperature, charge disordered phase and the low temperature charge-ordered phase. At lower densities we expect stability of the bcc solid when the temperature is low, and a first order transition to the liquid phase when the temperature is increased. The bcc solid coexists with ion-diluted ("gas") phase at very low T and with a liquid phase at higher T. We have identified the fluctuation-induced first-order transition between fluid and the charge-ordered phase with the liquid - charge-ordered bcc-solid coexistence. Further studies are necessary to determine high-density, high temperature three-phase equilibria for the liquid, charge-ordered bcc, charge-ordered fcc, and charge-disordered fcc phases. Figure 7 shows two possibilities. Note that the diagram shown in Fig. 7(A) is similar to the diagram found in simulations for the RPM in continuum space [17]. This shows that model I is indeed similar to the continuum system, and that our approch permits a prediction of the phase behavior for the whole range of concentrations of ions within the same formalism.

ACKNOWLEDGMENTS

We gratefully acknowledge the support of the Division of Chemical Sciences, Office of the Basic Energy Sciences, Office of Energy Research, U.S. Department of Energy. The work of A.C. was partially funded by the KBN Grant No. 1 P03B 033 26.

APPENDIX: LATTICE COULOMB POTENTIAL

The lattice Coulomb potential is a solution of the discretized Poisson-Boltzmann equation, and in Fourier representation assumes the form

$$\tilde{V}_c(\mathbf{k}) = \frac{2\pi}{3[1-\tilde{f}_{\text{latt}}(\mathbf{k})]}, \tag{A1}$$

where the index latt denotes the sc, fcc, or the bcc lattice. The lattice characteristic function $\tilde{f}_{\text{latt}}(\mathbf{k})$ depends on the kind of the lattice. For the sc, fcc and bcc lattices $\tilde{f}_{\text{latt}}(\mathbf{k})$ is given by

$$\tilde{f}_{\text{sc}} = \frac{1}{3}\sum_{i=1}^{3} \cos k_i, \tag{A2}$$

$$\tilde{f}_{\text{fcc}}(\mathbf{k}) = \frac{1}{3}\sum_{i<j} \cos k_i \cos k_j, \tag{A3}$$

and

$$\tilde{f}_{\text{bcc}}(\mathbf{k}) = \prod_{i=1}^{3} \cos k_i, \tag{A4}$$

respectively. The constants V_0^{latt} and V_1^{latt} are defined via equations

$$V_0^{\text{latt}} = \int_{\mathbf{k}} \frac{1}{3[1-\tilde{f}_{\text{latt}}(\mathbf{k})]}, \tag{A5}$$

$$V_1^{\text{latt}} = \int_{\mathbf{k}} \frac{\cos k_1}{3[1-\tilde{f}_{\text{latt}}(\mathbf{k})]}. \tag{A6}$$

The values we need in this work are:

$$V_0^{\text{sc}} \approx 0.5055, \quad V_0^{\text{fcc}} \approx 0.4482, \quad V_0^{\text{bcc}} \approx 0.465, \tag{A7}$$

$$V_1^{\text{sc}} \approx 0.172. \tag{A8}$$

[1] A. Ciach and G. Stell, J. Mol. Liq. **87**, 253 (2000).
[2] B. Hafskjold and G. Stell, in *The Liquid State of Matter. Fluids, Simple and Complex*, edited by E. N. Montroll and J. L. Lebowitz (North Holland, Amsterdam, 1982).
[3] G. Stell, Phys. Rev. A **45**, 7628 (1992).
[4] G. Stell, J. Stat. Phys. **78**, 197 (1995).
[5] M. Kleemeier, S. Wiegand, W. Schröer, and H. Weingärtner, J. Chem. Phys. **110**, 3085 (1999).
[6] E. Luijten, M. E. Fisher, and A. Z. Panagiotopoulos, J. Chem. Phys. **114**, 5468 (2001); E. Luijten, M. E. Fisher, and A. Z. Panagiotopoulos, Phys. Rev. Lett. **88**, 185701 (2002).
[7] G. Stell, in *New Approaches to Problems in Liquid-State Theory*, edited by C. Caccamo, J.-P. Hansen, and G. Stell (Kluwer Academic Publishers, Dordrecht, 1999).
[8] R. Dickman and G. Stell, *Proceedings of the Conference Treatment of Electrostatic Interactions in Computer Simulations of Condensed Media* (Santa Fe, July 1999), edited by G. Hummer and L.R. Pratt (AIP, New York, 1999).
[9] J. S. Høye and G. Stell, J. Stat. Phys. **89**, 177 (1997).
[10] A. Z. Panagiotopoulos and S. K. Kumar, Phys. Rev. Lett. **83**, 2981 (1999).
[11] A. Ciach and G. Stell, Phys. Rev. Lett. **91**, 060601 (2003).
[12] J. L. Lebowitz and J. K. Percus, Phys. Rev. **144**, 251 (1966).
[13] B. Jancovici, Physica (Amsterdam) **31**, 1017 (1965).
[14] D. S. Gaunt and M. E. Fisher, J. Chem. Phys. **43**, 2840 (1965).
[15] F. Bresme, C. Vega, and J. L.F. Abascal, Phys. Rev. Lett. **85**,

3217 (2000).
[16] N. G. Almarza and F. Encisco, Phys. Rev. E **64**, 042501 (2001).
[17] C. Vega, J. L.F. Abascal, and C. McBride, J. Chem. Phys. **119**, 964 (2003).
[18] V. Kobelev, A. B. Kolomeisky, and M. E. Fisher, J. Chem. Phys. **116**, 7589 (2002).
[19] A. Brognara, A. Parola, and L. Reatto, Phys. Rev. E **65**, 066113 (2002).
[20] A. Ciach and G. Stell, J. Chem. Phys. **114**, 3617 (2001).
[21] A. Ciach and G. Stell, J. Chem. Phys. **114**, 382 (2001).
[22] A. Ciach and G. Stell, Physica A **306**, 220 (2002).
[23] C. W. Outhwaite, *Statistical Maechanics. A Specialist Periodic Report*, edited by K. Singer (The Chemical Society, London, 1975), Vol. 2, p. 188.
[24] S. A. Brazovskii, Sov. Phys. JETP **41**, 85 (1975).
[25] T. L. Hill, *Statistical Mechanics. Principles and Selected Applications* (McGraw-Hill, New York, 1956).
[26] Y. Levin, C. J. Mundy, and K. A. Dawson, Phys. Rev. A **45**, 7309 (1992).
[27] G. H. Fredrickson and E. Helfand, J. Chem. Phys. **87**, 697 (1987).
[28] P. Viot and G. Tarjus, Europhys. Lett. **44**, 423 (1998).
[29] M. Grousson, G. Tarjus, and P. Viot, Phys. Rev. E **64**, 036109 (2001).
[30] A. Ciach (unpublished).